

Analysis of Ion-Pairing in Solid State and Solution in *p*-cymene ruthenium complexes. Anion- dependent cytotoxicity.

Marta Martinez-Alonso,¹ Pedro Sanz,² Paula Ortega,² Gustavo Espino,^{1} Félix A. Jalón,²
Mairena Martín,² Ana M. Rodriguez,³ José A. López,⁴ Cristina Tejel,^{4*} Blanca R. Manzano,^{2*}*

¹ U. de Burgos. Departamento de Química, Facultad de Ciencias. Plaza Misael Bañuelos s. n.,
09001-Burgos, Spain.

² U. de Castilla-La Mancha. Departamento de Química Inorgánica, Orgánica y Bioquímica.
IRICA. Fac. de Ciencias y Tecnologías Químicas, Avda. C. J. Cela, 10, 13071-Ciudad Real,
Spain.

³ U. de Castilla-La Mancha. Departamento de Química Inorgánica, Orgánica y Bioquímica.
IRICA. Escuela Técnica Superior de Ingenieros Industriales. Avda. C. J. Cela, 3, 13071-Ciudad
Real, Spain.

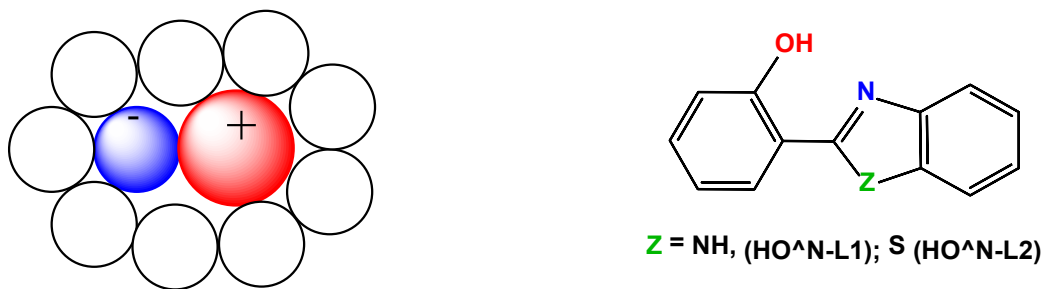
⁴ Departamento de Química Inorgánica, Instituto de Síntesis Química y Catálisis Homogénea
(ISQCH), CSIC-Universidad de Zaragoza, Pedro Cerbuna 12, 50009-Zaragoza, Spain.

ABSTRACT: The importance of ion-pairing in different fields of chemistry is widely recognized. In this work we have synthesized a set of cationic *p*-cymene ruthenium complexes of general formula $[(p\text{-cym})\text{Ru}(\text{L}')(\kappa^2\text{-O}^{\wedge}\text{N-L})]\text{X}$ (*p*-cym = *p*-cymene; L' = N-methylimidazole (MeIm), N-ethylpiperidylimidazole (EpiIm), 1,3,5-triaza-7-phosphaadamantane (PTA); L = 2-(1H-benzimidazol-2-yl)phenolato (L1), 2-(1,3-benzothiazol-2-yl)phenolato (L2); X = Cl[−], BF₄[−], OTf[−], BPh₄[−]). X-ray diffraction studies on selected complexes revealed relatively strong anion-cation interactions in the solid state mainly based on N–H[⋯]X (X = Cl, F, O) and C–H[⋯]π interactions, also observed in the DFT-modelled complexes in the gas phase. Moreover, NMR studies showed that they exist as intimate ion-pairs in solution and remarkably, as head-to-tail quadruples in the particular case of the cation $[(p\text{-cym})\text{Ru}(\text{RIm})(\kappa^2\text{-O}^{\wedge}\text{N-L1})]^+$ ([1]⁺) with Cl[−] and BPh₄[−] as counteranions. Furthermore, a value of $\Delta G = -2.9 \text{ kcal mol}^{-1}$ at 299 K has been estimated for the equilibrium $\{[1]\text{BPh}_4\cdots[1]\text{BPh}_4\} \rightleftharpoons 2 \{[1]^+\cdots\text{BPh}_4^-\}$ in concentrated CDCl₃ solutions. In addition, preliminary studies aimed to establish structure-activity relationships concerning the cytotoxic properties against HeLa cell lines of the derivatives suggested a clear positive effect derived from the presence of the lipophilic BPh₄[−] anion and also from the NH group of the benzimidazolyl fragment.

INTRODUCTION

The importance of ion-pairing effects on properties of ionic compounds has been recognized in different disciplines of chemistry.¹ When one or more of the ions is a transition metal coordination compound,² such ion-pairs have practical importance in catalysis,^{2–5} stoichiometric reactions,² supramolecular assembly,^{6–11} charge transfer in solution^{12,13} and chromatography,¹⁴ among others. According to Macchioni,² ion pairs are defined as pairs of oppositely charged ions, with a common solvation shell, held together prevalently by Coulombic forces with (a) lifetimes sufficiently longer than the correlation time of Brownian motion (kinetic stability) and (b) a binding energy higher than kT (thermodynamic stability). An ion pair in which no solvent molecules interposes between the two ions is called a “contact ion pair” (alternatively intimate or tight ion pair) (Chart 1). This is opposed to “loose” solvent separated ion pairs. Traditional techniques to study ion-pairing include X-ray crystallography,¹⁵ electrical conductivity, dielectric or ultrasonic relaxation,^{1,16} UV-visible¹⁷ and NMR spectroscopy. This later technique is being explored more intensely in recent years to study the formation of ion-pairs in solution and includes 2D correlation studies as 2D correlation studies based on nuclear Overhauser effect (NOESY or ROESY), Diffusion Ordered Spectroscopy (DOSY) and also the analysis of displacement in peak position that can render information about the sites involved in the ion-pairing interactions.^{18–23} In the case of cations of transition-metal complexes, the interaction in a contact ion-pair takes place between the anion and the ligands.²⁴ Besides the electrostatic attraction, other non-covalent interactions^{10,25} such as hydrogen bonds,^{9,26–30} stacking,³¹ anion $\cdots\pi$,³² X–H $\cdots\pi$ interactions^{33–36} (also considered as improper hydrogen bonds),²⁵ and hydrophobic contacts (in aqueous systems) may contribute to the anion-cation interaction. Some of these interactions may lead to a specific anion cation relative orientation.

Chart 1. Contact ion-pair (left) and proligands used in this work (right).



In the research field of metal-based chemotherapy or diagnosis, ionic complexes are frequently used and their counterions are usually considered as merely spectators in their biological activity.³⁷ Besides, the lipophilic nature of the biological membranes restricts the direct uptake of positively charged hydrophilic metal complexes. The inclusion of hydrophobic ligands³⁸ or the conjugation to proteins has been addressed to overcome this problem.³⁹ An easy alternative is the use of lipophilic counteranions that can form neutral entities through ion-pairing to facilitate transportation across the lipophilic membrane. An anion of high lipophilicity is BPh_4^- (tetraphenylborate), which provides high solubility in non-polar solvents to its salts. Moreover, it has been described that this anion is able to improve drug uptake and toxicity of organic hydrophobic ammonium or pyridinium salts that inhibit the respiratory process of mitochondrias,⁴⁰⁻⁴² while BPh_4^- alone exhibited nearly no effect.⁴³ In the field of metal-based chemotherapy, a work by Williams et al. has reported an increased cytotoxicity for Cp^*Ru complexes containing the BPh_4^- anion versus BF_4^- or PF_6^- ⁴⁴ and very recently, Castonguay has found improved antiproliferative effect in benzene-Ru complexes with this anion.^{45,46} Liu et al. also found a great influence of the counterion in the anticancer activity of Cp^*Ir complexes, but in this case the hydrophobic anions BPh_4^- or BArF^- ($[\text{3,5-(CF}_3)_2\text{Ph}]_4\text{B}^-$) led to lower activity.⁴⁷ However, in the cases described of positive effect of the BPh_4^- anion in the biological properties,

the anion-cation interaction in solution has not been studied, with the exception of a ROESY spectra that reflected interaction of the phenyl groups of the anion and the benzene ring in an arene Ru complex.⁴⁶

When structures of BPh_4^- salts have been determined by X-ray diffraction, $\text{X-H}\cdots\pi$ interactions with the arene rings of the anion acting as hydrogen acceptors and H atoms of the ligands are very frequently found.⁴⁸⁻⁵² The interaction is charge assisted due to the negative charge of the anions and the positive charge spread all over the ligands by coordination to the metal cation.⁴⁸

In this paper we report on the synthesis of several monocationic *p*-cymene ruthenium derivatives containing both a neutral monodentate ligand (some of them containing an imidazolyl ring) and a N^O anionic ligand 2-(1H-benzimidazol-2-yl)phenolato or 2-(1,3-benzothiazol-2-yl)phenolato, see Chart 1 for the corresponding pro-ligands) and different counteranions (Cl^- , BF_4^- , OTf^- , BPh_4^-). The main objective has been to analyse the influence of the type of counteranion and the presence of different functional groups in the anionic ligand (N-H or S) on the formation of ion-pairs in solution and in the cation-anion relative orientation. The analysis of a possible correlation between the ion-pairing in solution and solid state is another objective of the work. The evaluation of a possible positive effect of the tetraphenylborate anion in their cytotoxic properties has also been addressed. Because of that, the Ru metallic centre was chosen considering the promising results of Ru complexes in chemotherapy.⁵³⁻⁶¹ The ligand L1 and imidazolyl derivatives were selected on the ground of previous anticancer activities in Ru complexes with these ligands^{62,56} and the substituents in the imidazolyl rings were introduced to have another hydrophobic point of interaction with the BPh_4^- anion, apart from the arene fragment. The ligand PTA was used to evaluate the effect of increasing water solubility. Besides the information concerning the formation of the ion-pairs, we have found the formation of

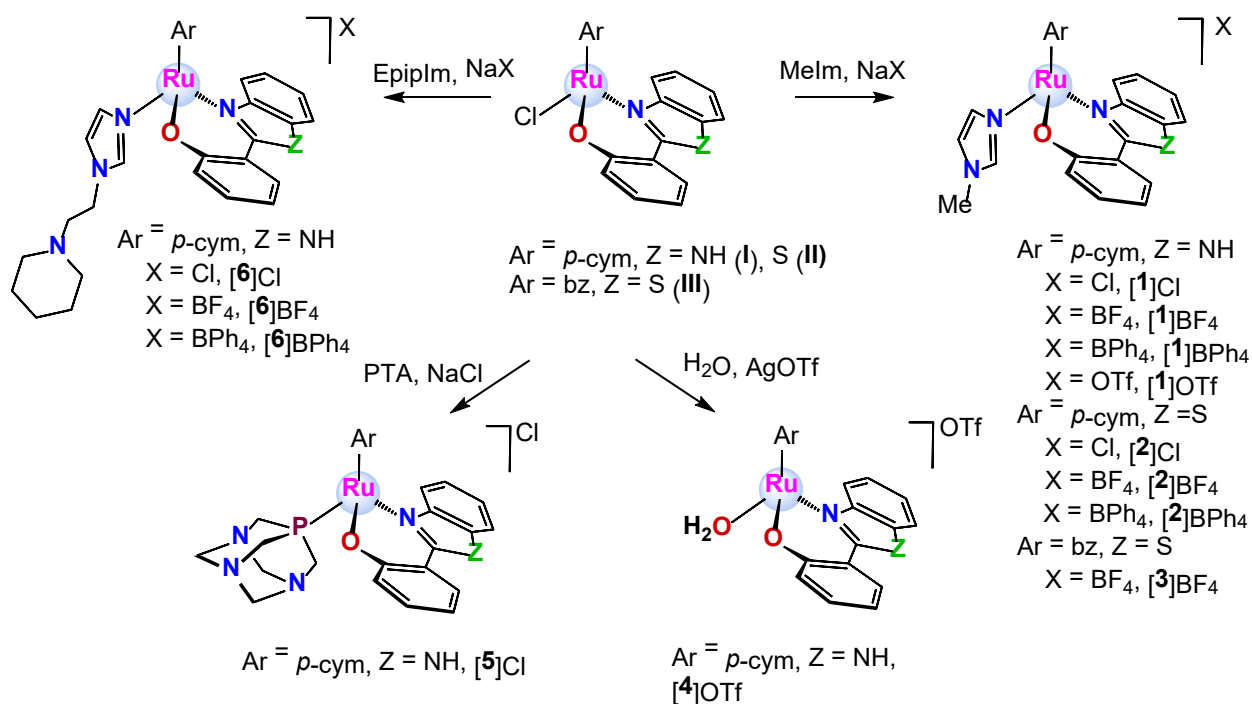
quadruples and the work also demonstrates the increase in the cytotoxic activity of the BPh_4^- derivatives in three different families of complexes.

RESULTS AND DISCUSSION

Synthesis of the complexes. The neutral chloride complexes **I-II** of general formula $[(p\text{-cym})\text{Ru}(\text{Cl})(\kappa^2\text{-O}^{\wedge}\text{N-L})]$ ($p\text{-cym}$ = p -cymene; L = L1 , L2) previously prepared by us,⁶³ were found to be useful precursor for the synthesis of the new cationic complexes depicted in Scheme 1. Thus, chloride replacement by the imidazole derivatives MeIm (N-methylimidazole) and EpipIm (N-ethylpiperidylimodazole) in the presence of a sodium salt (NaCl , NaBF_4 or NaBPh_4) yielded $[(p\text{-cym})\text{Ru}(\kappa^2\text{-O}^{\wedge}\text{N-L})(\text{MeIm})]^+$ ($\text{L} = \text{L1}$ (**[1]**⁺), L2 (**[2]**⁺), and $[(p\text{-cym})\text{Ru}(\kappa^2\text{-O}^{\wedge}\text{N-L1})(\text{EpipIm})]^+$ (**[6]**⁺), which were isolated as the corresponding Cl^- , BF_4^- , and BPh_4^- salts. Reactions with EpipIm took place at room temperature whereas refluxing of methanol was required for those with MeIm. In a similar way, reaction of the benzene precursor $[(\text{bz})\text{Ru}(\text{Cl})(\kappa^2\text{-O}^{\wedge}\text{N-L2})]$ (**III**) with MeIm and NaBF_4 produced $[(\text{bz})\text{Ru}(\kappa^2\text{-O}^{\wedge}\text{N-L2})(\text{MeIm})]\text{BF}_4$ (**[3]** BF_4).

The triflate derivatives having MeIm or water as ligands, $[(p\text{-cym})\text{Ru}(\kappa^2\text{-O}^{\wedge}\text{N-L1})(\text{MeIm})]\text{OTf}$ (**[1]** OTf) and $[(p\text{-cym})\text{Ru}(\kappa^2\text{-O}^{\wedge}\text{N-L1})(\text{OH}_2)]\text{OTf}$ (**[4]** OTf) were synthesized from **I** and an excess of AgOTf in the presence of MeIm or using a mixture of ethanol/water (ratio 1/1), respectively. The phosphane compound $[(p\text{-cym})\text{Ru}(\kappa^2\text{-O}^{\wedge}\text{N-L1})(\text{PTA})]\text{Cl}$ (**[5]** Cl) was obtained from the reaction of **I** with the water-soluble phosphane 1,3,5-triaza-7-phosphaadamantane (PTA) at room temperature.

Scheme 1. Synthesis of the complexes.



All the complexes were isolated in good yields (from 73% to 95%) and fully characterized by analytical and spectroscopic methods including X-ray diffraction studies on complexes $[\mathbf{1}]\text{BPh}_4$, $[\mathbf{3}]\text{BF}_4$, $[\mathbf{5}]\text{Cl}$, and $[\mathbf{6}]\text{BPh}_4$. The products were obtained as racemic mixtures of the two possible enantiomers as the result of chirality on the metal ion (R_{Ru} and S_{Ru}) due to the asymmetry of the bidentate ligand.

The aqueous solubility of the complexes was measured. The results are gathered in Table 1. As expected, the highest solubility value is found for the PTA complex $[\mathbf{5}]\text{Cl}$. The comparison of the values for $[\mathbf{1}]\text{Cl}$ and $[\mathbf{2}]\text{Cl}$, on one side, and $[\mathbf{1}]\text{BF}_4$ and $[\mathbf{2}]\text{BF}_4$, on the other, reflects a higher solubility for the complexes with the O^N-L1 ligand than for those containing O^N-L2. The decrease in the solubility values when Cl^- is replaced by OTf^- or BF_4^- is assigned to the high hydration energy of the Cl^- anion.⁶⁴ The presence of the less hydrophobic benzene ring in $[\mathbf{3}]\text{BF}_4$

compared to *p*-cymene in [2]BF₄ leads to a higher solubility of the former.⁶⁵ The solubility of complexes with the hydrophobic anion BPh₄[−] is below 0.2 mM.

Table 1. Solubility data in water (mM) of the new complexes, at room temperature.

[5]Cl	[1]Cl	[6]Cl	[6]BF ₄	[3]BF ₄	[1]BF ₄	[2]Cl	[2]BF ₄	[1]OTf
22.0	10.9	5.3	3.1	2.5	2.4	1.7	1.3	1.1

Plausible hydrolysis reactions leading to the extrusion of MeIm and PTA were evaluated analysing the evolution of solutions of complexes [1]OTf and [5]Cl in D₂O by ¹H NMR. Spectra were recorded for solutions (1.1 mM for [1]OTf and 3 mM for [5]Cl) of the complexes at different times (30 min and 24 h), and afterwards in the presence of NaCl, mimicking the physiological conditions as model concentrations for the intracellular (5 mM) and blood plasma conditions (100 mM) (see below).⁶⁶ No changes in the ¹H NMR spectra were observed with the exception of the expected disappearance of the NH resonance, reflecting robust MeIm–Ru and PTA–Ru bonds against aquation under physiological conditions. Nonetheless, the H^a proton of the imidazolyl ring reduced its intensity after four weeks. This fact is attributed to a deuteration process, a fact that reflects its acidity, probably as a consequence of the coordination of the imidazole ring.

Structural Characterization by X-ray diffraction methods. Figure 1 displays the molecular structures of the cations [1]⁺, [3]⁺, [5]⁺, and [6]⁺, whereas selected bond distances angles are shown in Table 2 (see Table S1 for crystal data). The four complexes crystalized in monoclinic

centrosymmetric space groups $P2_1/n$ or $P2_1/c$, so that both enantiomers are in the crystal. Only one of them is shown in Figure 1.

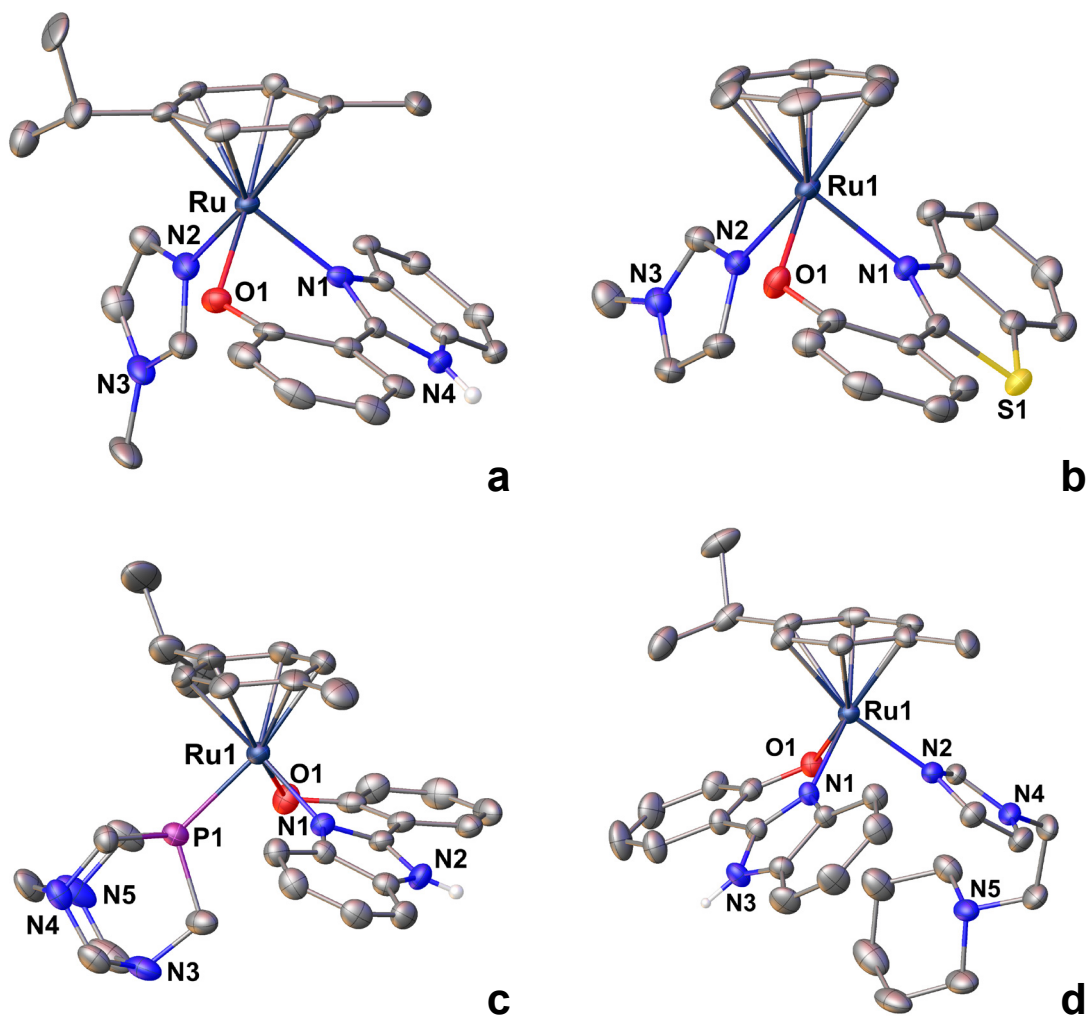


Figure 1. Molecular structures (ORTEP at the 30% level) of the cations: a) $[(p\text{-cym})\text{Ru}(\kappa^2\text{-O}^{\wedge}\text{N-L1})(\text{MeIm})]^+$ [**1**]⁺, b) $[(\text{bz})\text{Ru}(\kappa^2\text{-O}^{\wedge}\text{N-L2})(\text{MeIm})]^+$ [**3**]⁺, c) $[(p\text{-cym})\text{Ru}(\kappa^2\text{-O}^{\wedge}\text{N-L1})(\text{PTA})]$ [**5**]⁺, and d) $[(p\text{-cym})\text{Ru}(\kappa^2\text{-O}^{\wedge}\text{N-L1})(\text{EpipIm})]^+$ [**6**]⁺ in complexes [**1**] BPh_4 , [**3**] BF_4 , [**5**] Cl , and [**6**] BPh_4 respectively. Anions, solvent molecules and hydrogen atoms except the NH protons have been omitted for clarity.

In the four cases, the ruthenium shows a three-legged piano-stool environment conformed by the η^6 -arene, and the chelate (N[^]O) and the monodentate ligands. The coordination bond distances lie in the expected range (close to 2 Å).^{67,68} The Ru–O (2.066–2.081 Å) and Ru–N bond distances (2.068–2.111 Å) of the chelate ligands are very similar in the different complexes with a longer distance for the Ru–N(benzothiazolyl) bond (complex ([3]BF₄), as it has been previously observed in **II** (see Scheme 1).⁶³ The Ru–N(RIm) distance (2.100–2.108 Å) is similar to those in related complexes reported in the literature.^{69,70} The Ru–C(average) and Ru–C(centroid) distances are very similar in the four complexes and are also standard.^{69,70} The bite angle N1–Ru–O1 is slightly higher for the complex with O[^]N-L2 (84.02(7) °) than for complexes with O[^]N-L1 ligand (82.1–82.9 °).

Table 2. Selected bond distances (Å) and angles (°) for the cations in [1]BPh₄, [3]BF₄, [5]Cl, and [6]BPh₄.

Atom1-Atom2	[1]BPh ₄	[3]BF ₄	[5]Cl	[6]BPh ₄
Ru–N1	2.072(4)	2.111(2)	2.068(3)	2.068(3)
Ru–O1	2.081(3)	2.066(2)	2.069(2)	2.072(2)
Ru–N2/P1	2.106(4)	2.108(2)	2.304(1)	2.100(3)
Ru–C (average)	2.190(5)	2.189(3)	2.205(4)	2.189(4)
Ru–Ct(arene)	1.67	1.68	1.70	1.68
N1–Ru–O1	82.1(1)	84.02(7)	82.4(1)	82.9(1)

Ct = centroid of the arene ring

In the four structures, the O[^]N chelate ring features a twisted envelope conformation. This is expected for six-membered metallacycles including at least one atom with sp³ hybridization (O

in this case). The phenolate and benzimidazolyl (or benzothiazolyl) fragments of O^N-L1 or O^N-L2 ligands are not coplanar and display dihedral angles ranging from 17 to 20 °.

The 3D crystal packing of [1]BPh₄ shows a N–H4^{···}π interaction between the anion and the benzimidazolyl unit and several C–H^{···}π interactions involving the BPh₄[−] anion that participates both as CH donor and π acceptor (see Table S2 and Figure 2, left). Noteworthy, a C–H^{···}π interaction involves the imidazole ring of the O^N-L1 ligand as π-acceptor, whereas another contains a proton of the methyl group of the MeIm ring as H donor. In addition, there are also C–H^{···}π interactions between the *p*-cymene ring and a second anion placed on the other side of the cation, alternating the roles of H donor and π-acceptor (see Figure S2). Moreover, the methanol crystallization molecules participate in the formation of hydrogen bonds.

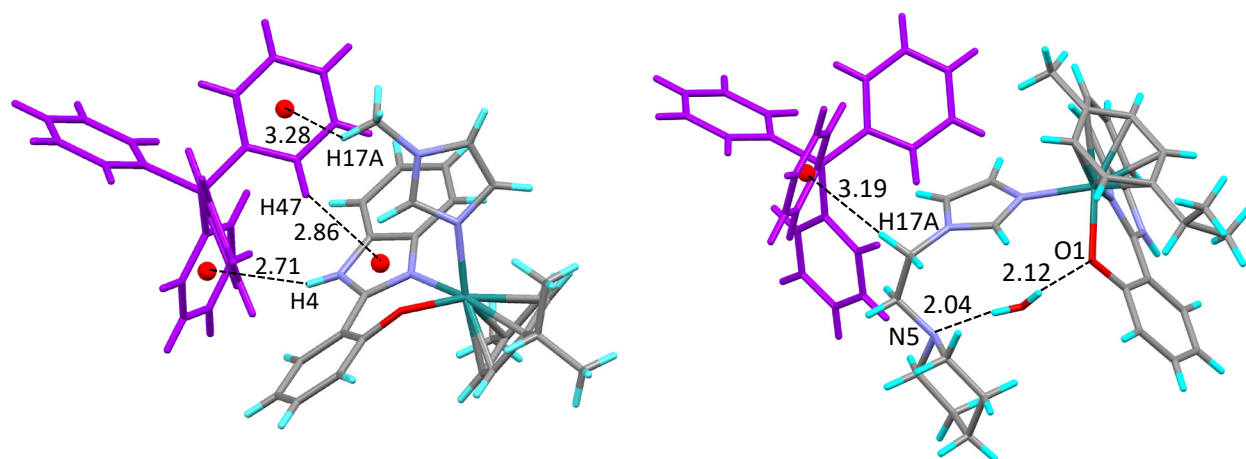


Figure 2. Anion-cation contacts and hydrogen interactions in [1]BPh₄ (left) and [6]BPh₄ (right).

For the related complex with the tetraphenylborate anion, [6]BPh₄, a C–H^{···}π interaction involving the BPh₄[−] anion was also observed, in such a way that one phenyl group of the anion participates as π-acceptor and the H17A proton as donor (EpipIm ligand). There are also

hydrogen interactions with the water molecule involving the O and N atoms of the phenoxy and piperidine rings, respectively (see Table S3 and Figure 2, right).

In the case of $[3]BF_4$, multiple C–H \cdots F hydrogen bonding interactions are observed where the anion connects six cations (see Table S3). The crystallization solvent molecules also participate in the formation of hydrogen bonds and a F \cdots S short contact is also observed with a distance of 3.130(4) Å, lower than the sum of the van der Waals radii (Figure S3).

In $[5]Cl$, the chloride anion stabilizes the crystal packing through the formation of hydrogen bonding interactions involving two different cations and the solvent molecules (Table S3). A short hydrogen bonding interaction is established with the NH group, whereas a weaker one is formed with the nearby H5 proton (Figure 3, right). A C–H \cdots π interaction between the proton H17B of the PTA ligand of one cation and the phenoxy ring of another cation is also observed (see Figure S4).

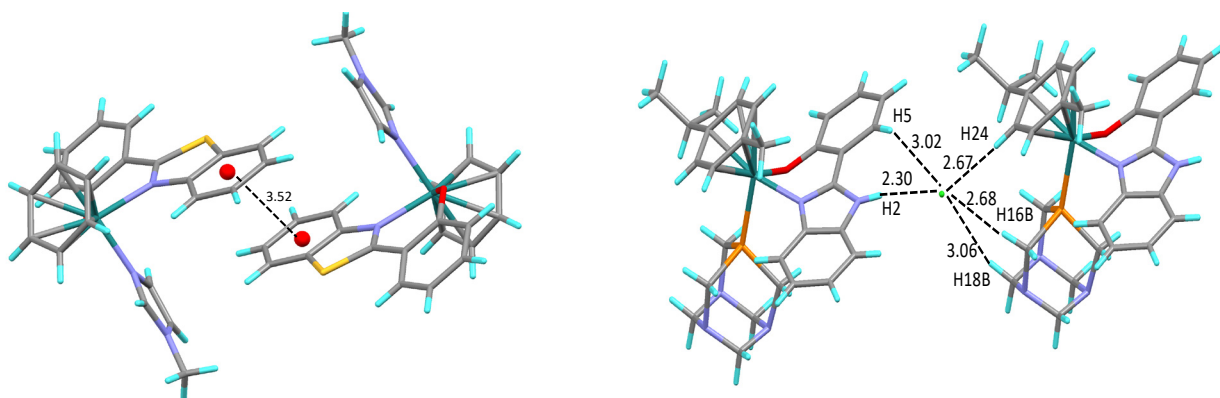


Figure 3. Anion-cation contacts and hydrogen interactions in $[3]BF_4$ (left) and $[5]Cl$ (right).

Complexes $[3]BF_4$, and $[5]Cl$ also feature a $\pi\cdots\pi$ stacking interaction between the six-membered rings of the benzothiazolyl or benzimidazolyl fragments, respectively, of two adjacent cations with a head to tail orientation (see Table S4 and Figures 3, left and S5).

Computational Studies. Additional information on anion-cation interactions was gathered from DFT studies (B3LYP-D3, 6-311G(d,p)/LanL2TZ(f)) on selected complexes. The modeled complex [1]BPh₄ reproduced very well the three main bonding interactions found in the solid state: N–H \cdots π (BPh₄), (ImMe)C–H \cdots π (BPh₄), and (BPh₄)C–H \cdots π (O[^]N–L1) (Figures S6 and S7, Table S5). The sole difference was that two protons of the methyl(Im) group (instead one) interact with one phenyl ring each one, which suggest a stronger (Me)CH \cdots π interaction in gas phase than that found in the solid state.

In complexes [1]Cl, [1]OTf, and [1]BF₄, a relatively strong N–H \cdots X (X = Cl, O, F) hydrogen bonding interaction⁷¹ was found in the three complexes, whereas those involving the adjacent H^{3'} proton (in [1]Cl) or the H^{a'} proton (in [1]OTf and [1]BF₄) was quite weak (Figure 4 and Table S6).

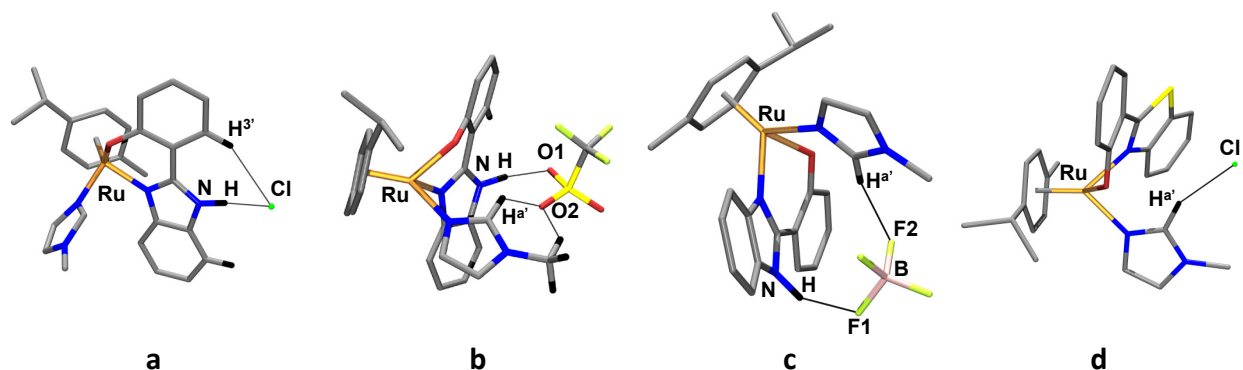
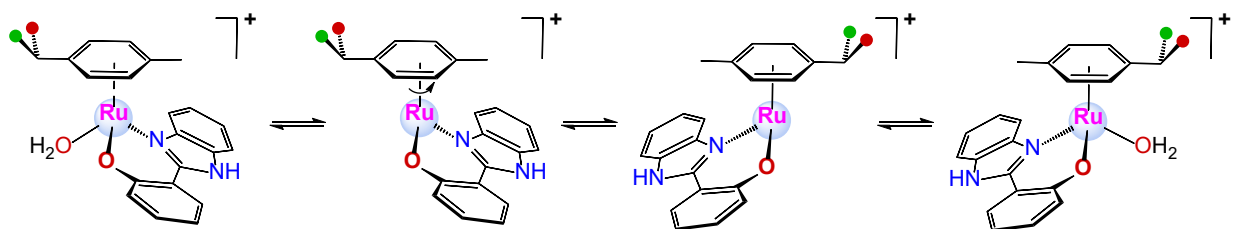


Figure 4. Anion-cation hydrogen interactions in the DFT-calculated (B3LYP-D3, 6-311G(d,p)/LanL2TZ(f)) structures of [1]Cl (a), [1]OTf (b), [1]BF₄ (c), and [2]Cl (d).

In the particular case of complex [2]Cl, which contains the O[^]N–L2 ligand the chloride anion was found to be interacting with the H^{a'} proton of the MeIm ring. Indeed, after coordination of the MeIm ligand to the ruthenium centre this proton is thought to become quite acid, a fact that should favour the formation of the mentioned hydrogen bond interaction.

NMR studies. In general terms, the cationic nature of the complexes agrees with the shift to low-field of almost all the proton resonances of the O[^]N-L1, O[^]N-L2, and *p*-cymene ligands relative to the neutral precursors **I-III**⁶³ (see Tables S7–S11 for a better comparison). In addition, the lack of symmetry of the complexes results in the display of two and four signals for the methyl groups of ^{*i*}Pr and the four aromatic protons, respectively, of the *p*-cymene ligand in the ¹H NMR spectra. An exception to this general trend was the aquo-complex **[4]OTf**, for which an apparent symmetry plane bisecting the *p*-cymene ligand was deduced from the observance of one singlet for the two methyl groups and only two signals for the aromatic protons in the ¹H NMR spectrum. An enantiomer's interconversion involving water decooordination, inversion at the ruthenium centre, and water re-coordination on the other side, along with the free rotation of the *p*-cymene ligand is proposed to account for these observations⁷² (Scheme 2).

Scheme 2. Plausible epimerization process in solution undergone by complex **[4]OTf.**

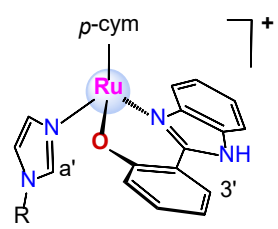


Because this process is not observed for the other complexes, it can be concluded that dissociation of the imidazole ligands in **[1]⁺–[3]⁺**, and **[6]⁺** or the phosphane PTA in **[5]⁺** does not occur, indicating relatively strong Ru–N(RIm) and Ru–P(PTA) bonds in the complexes (see below for hydrolysis studies).

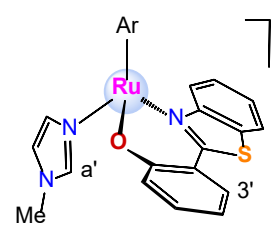
Particular attention was devoted to the elucidation of the anion-cation interactions in solution described above through the analysis of selected resonances in the ^1H NMR spectra.

i) NH proton. The participation of this proton in $\text{N-H}\cdots\text{X}$ ($\text{X} = \text{Cl}, \text{O}, \text{F}$) bond interactions can be established from its chemical shift, since such interactions usually lead to a decrease of its electron density that results in a low-field shifting in the ^1H NMR spectra.^{12,26,28,29,65,66} As shown in Table 3, a low-field shifting relative to the neutral complex **I** ($\delta = 10.67$ ppm)⁶³ is observed in all the cases, with the chloride complexes showing the more deshielded NH protons. This observation is in full agreement with the stronger ability of Cl^- as a hydrogen bonding acceptor relative to the other counter-anions.^{17,73}

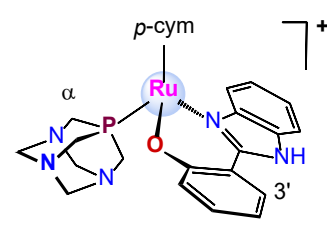
Table 3. Chemical shifts^a for selected ^1H NMR resonances of $[1]^+$, $[2]^+$, $[3]^+$, $[5]^+$, and $[6]^+$.



$\text{R} = \text{Me}, [1]^+; \text{Epip}, [6]^+$



$\text{Ar} = p\text{-cym}, [2]^+; \text{bz}, [3]^+$



$[5]^+$

	$[5]\text{Cl}$	$[1]\text{Cl}^b$	$[6]\text{Cl}^b$	$[1]\text{BF}_4^b$	$[1]\text{OTf}$	$[6]\text{BF}_4^b$	$[2]\text{Cl}^b$	$[3]\text{BF}_4$	$[2]\text{BF}_4$
NH	14.81	14.43	14.70	12.17	12.16	11.40	---	---	---
$\text{H}^{3'}$	8.43	8.35	8.28	7.88	7.88	7.81	7.56	7.59	7.57
$\text{H}^{a'}$	---	7.97	8.21	7.78	7.70	8.03	9.95	8.97	8.75

^a CDCl_3 , in ppm. ^b 30 mM.

ii) $\text{H}^{3'}$ proton. As deduced from the afore-mentioned DFT-studies, the formation of $\text{N-H}\cdots\text{X}$ ($\text{X} = \text{Cl}, \text{O}, \text{F}$) interactions in complexes with the $\text{O}^{\wedge}\text{N-L1}$ ligand is accompanied by one additional interaction of the close $\text{H}^{3'}$ proton with the counter-anion. This is also observed in the

X-ray structure of [5]Cl (Figure 3 right). Such interaction is again reflected in a low-field shifting of this proton, which accordingly, follows a similar trend than that observed for the NH proton (Table 3). Conversely, in complexes that lack the NH group, as those containing the chelating O[^]N-L2 ligand, this H^{3'} proton remains at *ca.* 7.58 ppm. Therefore, the N–H^{3'}⋯X interaction remains in solution (at least in some extension) for complexes in Table 3.

iii) *H^{a'} proton.* For complexes with the S-ligand, O[^]N-L2, the expected C–H^{a'}⋯X interaction (X = Cl, F, Figure 4) is associated to a low-field shift of this proton (Table 3). This shift is noticeable for [2]Cl, which agrees with the presence of a relatively tight ion-pair in CDCl₃ solutions. This interaction was observed for complexes [1]BF₄, [1]OTf and [2]Cl according to the DFT-modelled complexes (Figure 4). Interestingly, in the particular case of the chloride complexes having the NH-ligand, O[^]N-L1, ([1]Cl and [6]Cl) the low-field shifting of this proton could well reflect the presence of at least trinuclear entities of the type ‘cation⋯anion⋯cation’ (as found for [5]Cl in the solid state, Figure 3 right), since after the formation of the N–H^{3'}⋯Cl interaction with the first cation, the C–H^{a'/α}⋯Cl interaction should take place with a second cation placed on the other side of the chloride. This additional interaction was found to be slightly stronger in [6]Cl, which shows the more deshielded H^{a'} proton.

iv) *BPh₄[−] anion.* The interactions of the cations [1]⁺, [2]⁺, and [6]⁺ with the BPh₄[−] anion were nicely detected by the high-field shifting of the involved protons of the cations, and agree with those observed in the DFT-modelled structure for [1]BPh₄ (Figure S6). Δδ chemical shifts for selected protons, calculated as the difference between the chemical shift in complexes with BF₄[−] and BPh₄[−] counter-anions, are shown in Figure 5. The three main anion-cation interactions in these complexes (see above) are clearly evidenced by the high-field shift of:

- the NH proton (involved in a relatively strong NH⋯π(BPh₄) interaction),

- the H^{d'}/Me protons as well as the H^{a'} proton located in the shielding cone of the phenyl groups (because of the ImR–H^{a'}⋯π(BPh₄) interaction), and
- the H²/H³ protons of the *p*-cymene ligand that point at a second anion placed on the other side of the cation and involved in C–H²⋯π(BPh₄) interactions.

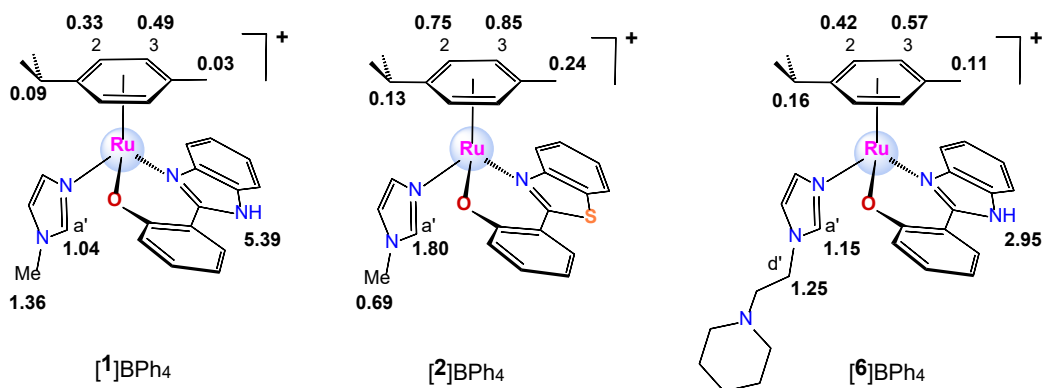


Figure 5. $\Delta\delta$ ^1H NMR chemical shifts, calculated as the difference between the chemical shift in complexes with BF_4^- and BPh_4^- counter-anions, for selected resonances of complexes $[\mathbf{1}]\text{BPh}_4$, $[\mathbf{2}]\text{BPh}_4$, and $[\mathbf{6}]\text{BPh}_4$.

The stronger shielding of the Me/H^{d'} protons in $[\mathbf{1}]^+$ and $[\mathbf{6}]^+$ compared to $[\mathbf{2}]^+$ suggest that the former interact in a stronger way with the anion placed on this part of the molecules, which can be attributed to the additional $\text{NH}\cdots\pi(\text{BPh}_4)$ interaction with this BPh_4^- anion (see Figure 2). Conversely, the H^{a'}, H² and H³ protons are more shielded in $[\mathbf{2}]^+$ than in $[\mathbf{1}]^+$ and $[\mathbf{6}]^+$, showing that the cation $[\mathbf{2}]^+$, which lacks the NH proton, interacts stronger with the anion placed on the other side as compared to $[\mathbf{1}]^+$ and $[\mathbf{6}]^+$.

In full agreement with these proposals, the ^1H , ^1H -NOESY spectrum of $[1]\text{BPh}_4$ showed the close proximity of the methyl protons of both, the MeIm and *p*-cymene ligands, to the H^o and H^m protons of the anion (Figure 6). Moreover, from the intensity of the signals, the methyl group in the MeIm seems to be closer to the anion than the methyl in the *p*-cymene ligand. These preferences for the relative cation-anion orientation are in contrast with the results reported for nitride chromium complexes where a lack of specificity in the interaction with BPh_4^- was found.²³

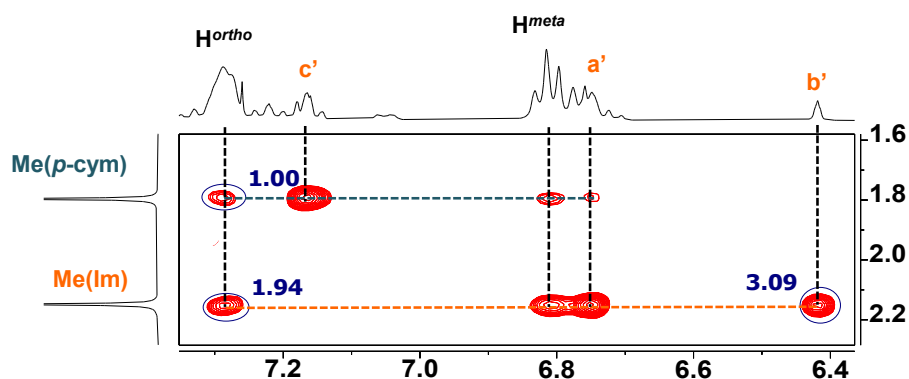


Figure 6. Selected region of the ^1H , ^1H -NOESY spectrum of $[1]\text{BPh}_4$ in CDCl_3 .

Furthermore, the evident effect of the anion on the position of some resonances of the cation was also verified recording the ^1H NMR spectrum of an equimolar mixture of $[1]\text{Cl}$ and $[1]\text{BPh}_4$ in CDCl_3 . Intermediate values for the chemical shifts between those observed for the separate complexes were observed, reflecting a situation of rapid interchange with respect the NMR time scale (see Figures S9 and S10).

The above mentioned data relative to the chemical shifts of selected protons strongly support the presence of intimate ion-pairs $\{[\text{Ru}]^+\cdots\text{A}^-\}$ in CDCl_3 solutions in all the cases, which were found to be stronger for those containing Cl^- and BPh_4^- as counter-anions. Moreover, for these

anions aggregates of even higher nuclearity were detected. In the chloride complexes, the anion interacts with two cations in a ‘cation⋯anion⋯cation’ sequence $\{[\text{Ru}]^+\cdots\text{Cl}^-\cdots[\text{Ru}]^+\}^+$. In the BPh_4^- counterparts, the observed sequence was found to be ‘anion⋯cation⋯anion’ $\{\text{A}^-\cdots[\text{Ru}]^+\cdots\text{A}^-\}$, since one part of the cation (NH, Me(Im)) interacts with one BPh_4^- anion while the opposite part (*p*-cymene) interacts with a different anion. In this regard, quadruple species such as $[\text{Ru}]\text{Cl}\cdots[\text{Ru}]\text{Cl}$ and $[\text{Ru}]\text{BPh}_4\cdots[\text{Ru}]\text{BPh}_4$, in which two tight ion pairs aggregate in a head to tail fashion, could well be the origin of the observed data.

Additional information supporting this picture was gathered from dilution experiments for the model complexes $[\mathbf{1}]\text{Cl}$ and $[\mathbf{1}]\text{BPh}_4$ in CDCl_3 . Such type of studies allowed to detect intimate ion-pairs, and even the existence of aggregates (*n* cations and *n* anions) as reported by Dupont et al,⁷⁴ Ammer et al,⁷³ and Macchioni et al,^{75–79} for example. In both cases, several ^1H NMR spectra were recorded from solutions 30 mM (whose ^1H NMR have been described above) up to 0.4 mM (see Tables S12 and S13). For the chloride complex variations in the chemical shifts of the involved protons NH, $\text{H}^{3'}$, $\text{H}^{\text{a}'}$ and H^2 are shown in Figure 7.

Dilution was accompanied by a high-field shifting of the $\text{H}^{\text{a}'}$ and H^2 protons involved in the interaction $[\mathbf{1}]\text{Cl}\cdots[\mathbf{1}]\text{Cl}$ between two ion-pairs, a clear indication of the cleavage of this interaction, since they move towards their usual chemical shifts in the absence of hydrogen bonds. At the same time, the NH and $\text{H}^{3'}$ protons, which participate in the single ionic-pair $\{[\mathbf{1}]^+\cdots\text{A}^-\}$ interaction, shift to the opposite sense (Table S12). These deshieldings can be easily understood because of the higher electronic density of the chloride when losing the interaction with the second cation. In other words, the disaggregation of $[\mathbf{1}]\text{Cl}\cdots[\mathbf{1}]\text{Cl}$ into the intimate ion-pair $\{[\mathbf{1}]^+\cdots\text{Cl}^-\}$ reinforces the intra anion-cation interaction in the later. Moreover, variations in the chemical shifts of the NH and $\text{H}^{\text{a}'}$ protons were found to be larger than those for the $\text{H}^{3'}$ and

H² protons. Clearly the more acidic NH and H^{a'} protons form stronger interactions with the chloride anion than the H^{3'} and H² protons.

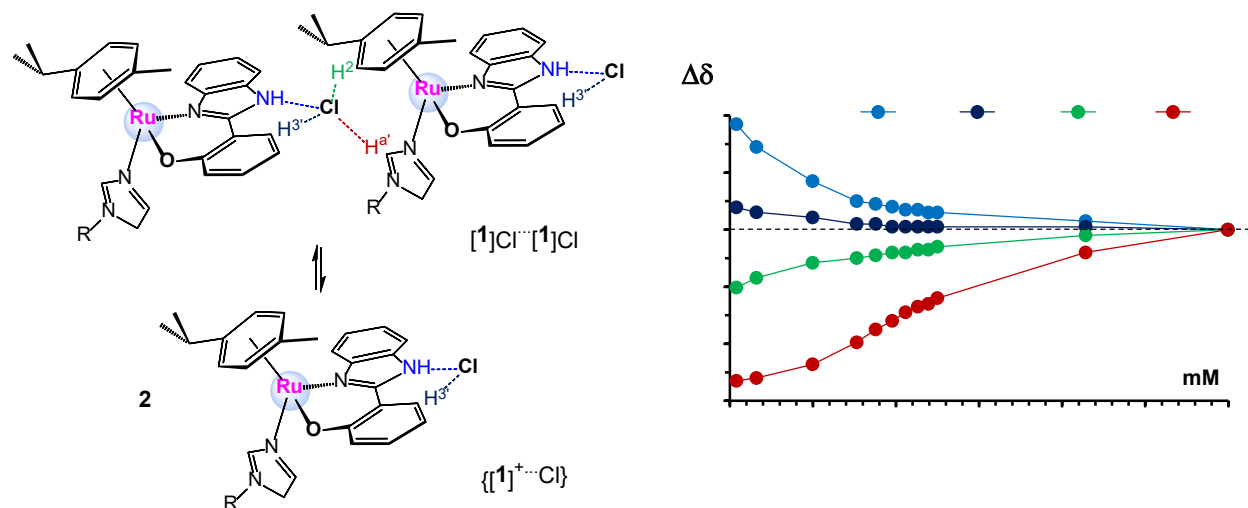


Figure 7. Equilibrium between quadruple species $[1]Cl \cdots [1]Cl$ and ion-pairs $\{[1]^+ \cdots Cl^-\}$ (left) and variation ($\Delta\delta$) of the 1H NMR chemical shifts for the NH, H^{3'}, H^{a'}, and H² protons for $[1]Cl$ versus concentration (right) in $CDCl_3$.

A similar behavior was observed for the related $[1]BPh_4$. As shown in Figure 8, protons of the *p*-cymene ligand shift towards low-field upon dilution according to the disaggregation of the quadruple assembly $[1]BPh_4 \cdots [1]BPh_4$ into the tight ion-pair $\{[1]^+ \cdots BPh_4^-\}$. This low-field shift is more relevant for the H³ proton and the methyl group, which indeed are those involved in $CH \cdots \pi$ interactions with the BPh_4^- anion (in green in Figure 8, see also Figure S12 and Table S13).

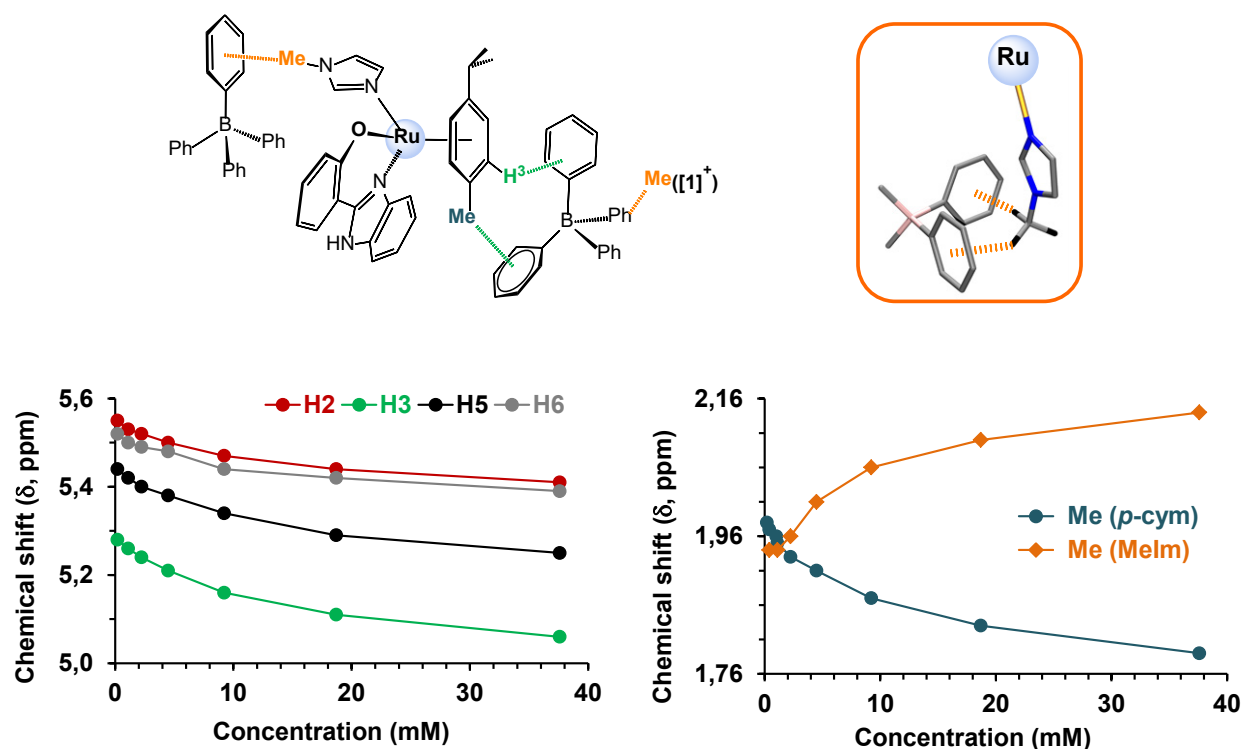


Figure 8. Plots of the variation of the 1H NMR chemical shifts of some resonances for $[1]BPh_4$ in $CDCl_3$, *versus* concentration. Chemical shifts of the aromatic protons of the *p*-cymene ligand are shown on the left and those for the methyl groups in *p*-cymene and Melm on the right. The inset shows the double (Me)CH $\cdots\pi$ interaction in the ionic-pair (H \cdots Ct = 2.457 and 2.449 Å from DFT).

Simultaneously, the methyl group of the methylimidazole undergoes a major shielding upon dilution evidenced by the shift to high-field (from $\delta = 2.14$ to 1.94 ppm, at 37.6 and 0.4 mM, respectively). This behaviour indicates that disaggregation of quadruple species through the equilibrium $\{[1]BPh_4 \cdots [1]BPh_4\} \rightleftharpoons 2 \{[1]^+ \cdots BPh_4^-\}$ reinforces the (Me)CH $\cdots\pi$ interaction in the tight ion-pair (in orange in Figure 8). In this case, cleavage of the interaction between two ionic-pairs (in green) allows to the BPh_4^- anion a slight rotation approaching a second phenyl group to

a second proton of the methyl group in MeIm (as found by DFT), which accounts for the high-field shifting of this methyl group upon dilution.

In order to corroborate this picture, the translational diffusion coefficients of the anion (D_t^-) and the cation (D_t^+) of [1]BPh₄ were estimated by performing pulsed-field gradient spin-echo (PGSE) NMR measurements at different concentrations (Table 4). The corresponding hydrodynamic radius (r_H^- and r_H^+) were then calculated using the modified Stokes-Einstein equation ($D_t = \frac{kT}{(f_s c) \pi \eta r_H}$), where the appropriate c factor: $c = \frac{6}{1+0.695b^{2.234}}$ ($b = \frac{r_{solv}}{r_H}$) was calculated by successive iterations.⁷⁵ In general terms, a value of the parameter $f_s = 1$ provides a good fitting, but because of the prolate-shape of the quadruple [1]BPh₄···[1]BPh₄ species, a value of 1.1 according to Perrin's equation,⁷⁶ was taken for the more concentrated solution (37.6 mM). The corresponding hydrodynamic volumes (V_H) were then obtained from the averaged hydrodynamic radii of the anion and cation assuming that they are spherical, and the aggregation number $N = \frac{V_H}{V_H^0}$ was estimated with $V_H^0 = 985 \text{ \AA}^3$ corresponding to the hydrodynamic volume at 2.24 mM, which contains the intimate ion-pair {[1]⁺···BPh₄⁻}. Indeed, this V_H^0 value (985 \AA^3) agrees quite well with those derived from the X-ray data (1014 \AA^3) and DFT-studies (973 \AA^3) for [1]BPh₄. This point has been corroborated by recording the ¹H NMR spectra at lower concentrations, where the resonance corresponding to the methyl group of MeIm remained at $\delta = 1.94$ ppm up to 0.2 mM, the lowest concentration available in our hands, which ensures the presence of the tight ion-pair.

Table 4. Diffusion coefficients ($10^{10} D_t \text{ m}^2 \text{ s}^{-1}$), hydrodynamic radii ($r_H \text{ \AA}$), hydrodynamic volume ($V_H \text{ \AA}^3$) and aggregation number (N) for complex [1]BPh₄ as a function of concentration (C , mM).

Entry	C	$D_t^{-\text{a}}$	r_H^{-}	$D_t^{+\text{b}}$	r_H^{+}	r_H	V_H	N^{c}
1	37.6	4.851	7.93	4.861	8.05	7.99	2136	2.17
2	18.7	5.702	7.55	5.685	7.73	7.64	1869	1.90
3	9.22	6.128	7.10	6.127	7.26	7.18	1549	1.57
4	4.49	6.455	6.79	6.535	6.89	6.84	1338	1.36
5	2.24	7.376	6.07	7.337	6.28	6.17	985	1.00

^a From the resonance of the H^{meta} protons of BPh_4^- . ^b Averaged of D_t obtained for the methyl groups of *p*-cymene and MeIm. ^c Calculated as $\frac{V_H}{V_H^0}$ where V_H^0 corresponds to the volume for the dilute solution, which contains the tight ion-pair [1]BPh₄.

Interestingly, at the highest concentration (entry 1) the aggregation number was found to be 2.17, which mainly corresponds to quadruple [1]BPh₄⋯[1]BPh₄ species, whereas the lowest concentration (entry 5) contains the tight ion-pair $\{[1]^+\cdots\text{BPh}_4^-\}$ as mentioned before. Remarkably, both cation and anion exhibit almost identical diffusion coefficients in all the available concentrations, so that we can conclude that they are diffusing through solution at the same rate. This represent an important point, since ensures that both, anion and cation, belong to the same aggregate and consequently, excludes the presence in the solution of odd ions (triples in this case) of the type $\{\text{BPh}_4\cdots[1]\cdots\text{BPh}_4\}^-\{[1]\}^+$, which otherwise are also compatible with the ¹H NMR spectra above described.

For the intermediate concentrations (entries 2-4) the equilibrium $\{[1]\text{BPh}_4\cdots[1]\text{BPh}_4\} \rightleftharpoons 2 \{[1]^+\cdots\text{BPh}_4^-\}$ accounts for the changes in the aggregation number N . Moreover, from the

volumes at 4.49 and 9.22 mM (entries 3-4), an averaged value for the K_{IQ} ⁷⁶ for this equilibrium of 132 ± 36 was obtained. It corresponds to $\Delta G = -2.9 \text{ kcal mol}^{-1}$ at 299 K and accordingly, that corresponding to the unobserved equilibrium: $[1]^+ + BPh_4^- \rightleftharpoons \{[1]^+ \cdots BPh_4^-\}$ should be higher.

The existence of quadruple species (or quadrupoles) in solution, although scarce, has been reported for some ruthenium complexes. As a matter of fact, they have been proposed for the octahedral complex $[Ru(PMe_3)_2(CO)(COMe)(k^2\text{-Pz}_2\text{-CH}_2)]BPh_4$ in a side by side (or head to head, $\{A[Ru] \cdots [Ru]A\}$) arrangement from $^1H, ^1H$ -NOESY data.⁷⁷ In addition, the complexes $[(p\text{-cym})Ru(H_2N(CH_2)_2NH_2)(Cl)]PF_6$ ⁷⁵ and $[(p\text{-cym})Ru(ArN=CM_2=CM_2=NAr)(Cl)]BF_4$ ⁷⁸ have also been reported as suitable to form ion-quadruples in head to head configuration. Conversely, a less coordinating anion such as BPh_4^- favors head to tail arrangements $\{A[Ru] \cdots A[Ru]\}$ as observed in $[(p\text{-cym})Ru(ArN=CM_2=CM_2=NAr)(Cl)]BPh_4$, the single precedent for fully characterized ion-quadruples in ruthenium chemistry.⁷⁹

Cytotoxicity. Preliminary studies of the cytotoxicity of some of the complexes were performed in HeLa (cervical carcinoma cell line) by means of an MTT cell viability assay. The values of IC_{50} (μM) are expressed in Table S14 (see also Figures S13-15).

The three precursors **I–III** were not active, nor the complexes containing ligand O^N-L2 or the complex with PTA as neutral ligand. Thus, in this series of complexes the presence of ligand O^N-L1, and perhaps more specifically the NH group, is necessary for the cytotoxic activity, at least against HeLa cell lines. The presence of the monodentate MeIm ligand exerted a positive effect. It was observed an effect of the anion present, as for example, with the better results obtained for **[1]**Cl than for **[1]**OTf but the most important conclusion is that in both $[1]^+$ and $[6]^+$, the presence of the BPh_4^- anion increased notably the anticancer activity. In fact, complex **[1]**BPh₄ was the most cytotoxic, with a value of IC_{50} even better than that of cisplatin both after

24 h ($IC_{50} = 16.3 \mu M$) and 48 h ($IC_{50} = 14.9 \mu M$). Complex [6]BPh₄ also exhibited relatively high antiproliferative effect. As stated, this effect of the BPh₄[−] anion in the cytotoxicity has already been reported in the literature in some ruthenium complexes.^{44,45,46}

Conclusions

Along this work we have showcased that semi-sandwich cationic ruthenium complexes of general formula [(*p*-cym)Ru(L')(κ^2 -O[^]N-L)]X show a great tendency to form tight ion-pairs in both, solid-state and solution. Complexes with Cl[−], OTf[−], and BF₄[−] as counter-anions, feature strong N–H \cdots X (X = Cl, O, F) bond interactions, whereas those having the lipophilic BPh₄[−] counter-anion mainly showed N–H \cdots π and C–H \cdots π bond interactions. These preferences suggest that the sites of ion-pairing can be controlled, at least, up to a certain extent. Moreover, a full agreement between X-ray and DFT-modelled structures was observed, which in addition showed a good correlation with the NMR studies concerning the chemical shift of the selected protons as well as dilution experiments. Interestingly, rare head-to-tail quadruple species were observed for complexes [1]Cl and [1]BPh₄ in concentrated CDCl₃ solutions. Furthermore, a value of $\Delta G = -2.9 \text{ kcal mol}^{-1}$ at 299 K has been estimated for the equilibrium $\{[1]BPh_4 \cdots [1]BPh_4\} \rightleftharpoons 2 \{[1]^+ \cdots BPh_4^-\}$.

Preliminary studies aimed to establish structure-activity relationships concerning the cytotoxic properties of the derivatives pointed out the existence of a clear positive effect of the presence of the lipophilic BPh₄[−] anion and also of the NH group of the benzimidazolyl fragment. The complex containing the PTA ligand was not active. An interesting aspect of the effect of the BPh₄[−] anion on the antiproliferative activity of metal complexes is that this simple approach

could be applicable to a range of cationic cytotoxic species and to the development of new formulations for metallo-drugs.

EXPERIMENTAL SECTION

General comments. All synthetic manipulations were carried out under nitrogen atmosphere (water- and oxygen free) using Schlenk techniques. The solvents, with the exceptions of water and ethanol, were distilled under nitrogen in the presence of the respective drying agents before its use or purified in a MBraun SPS MB-SPS-800 from commercial HPLC solvents. Deuterated solvents were deoxygenated by applying freezing-vacuum cycles and introducing a dry nitrogen atmosphere. Occasionally, some of them were also dried with molecular sieve (MS). The elemental analyses were performed in a LECO CHNS-932 or Thermo Quest FlashEA 1112 microanalyzers. Medium infrared spectra were recorded in a Nicolet Impact 410, in a Jasco FT/IR-4200 and in a Shimadzu IR Prestige-21 infrared spectrometer equipped with a Pike Technologies ATR. Samples were prepared either in KBr pellets (refraction) or with an ATR accessory (reflexion) and spectra were recorded with 32 or 64 scans, respectively, and a resolution of 4.0 cm^{-1} . Data were treated with Spectra Manager v.2.10.01 (Build 1). The FAB⁺ mass spectrometry measurements were obtained with a Thermo MAT95XP mass spectrophotometer with a magnetic sector. NMR spectra were registered with a VARIAN UNITY INOVA, VARIAN INOVA and Bruker Advance operating at 400, 500 and 500 MHz, respectively. Both monodimensional (^1H , ^{31}P , ^{19}F and ^{13}C) and bidimensional (^1H , ^1H gCOSY, ^1H , ^1H ROESY, ^1H , ^{13}C gHSQC and ^1H , ^{13}C gHMBC) experiments were recorded using standard sequences. A combined analysis of them allowed the accurate assignation of all protons and

carbons in the complexes. Chemical shifts, in ppm, are related to TMS (for ^1H and ^{13}C), CFCl_3 (for ^{19}F) and H_3PO_4 (for ^{31}P). The spectra were usually recorded at 25 °C and with 32 scans (for ^1H) and processed with MestReNova v10.0.2-15465. In the NMR analysis s, d, t, sept, m, and br denote singlet, doublet, triplet, septuplet, multiplet, and broad signal, respectively and *o*, *m*, *p* and *i* stands for *ortho*, *meta*, *para* and *ipso* positions of the phenyl rings. DOSY experiments were carried out using the PFGSE (Pulsed-Field Gradient Spin-Echo) NMR Diffusion methods and analysed with the software implemented by Bruker on a NMR AV500 spectrometer. The variation of the intensity of one selected signal in the ^1H NMR spectrum (I) is related to the strength of the gradient (G) by the following equation: $\text{Ln}(I/I^0) = -\gamma^2 \delta^2 G^2 (\Delta - \delta/3) D$, where γ = gyromagnetic ratio of the proton, δ = length of the gradient pulse, G = gradient strength, Δ = delay between the midpoints of the gradients, and D = diffusion coefficient.⁸⁰ Before recording the DOSY experiment, the values of δ (small delta) and Δ (big delta) were optimized for each complex by using the 1D sequence for diffusion measurements (stebpgp1s1d, δ (2 x P30) and Δ (d20), Bruker's software). The selected values provided a considerable reduction of the intensity of the signal, but it remained strong enough to be integrated. Next, the bidimensional DOSY experiment (stebpgp1s sequence) was recorded with the optimized δ and Δ values, varying G along 32 spectra. The data were analyzed with the Bruker's software, which provided directly the diffusion coefficient (D). The quality of the data were tested by representation $\text{Ln}(I/I^0)$ versus G^2 , which gave an excellent fit to a straight line in all the cases. Hydrodynamic radii (r_H) were calculated from the modified Stokes–Einstein equation according bibliography.⁷⁵ Temperature was previously calibrated by using a reference tube with ethylene glycol (80%) in $\text{dms}-d_6$. Chemical-shift separation (Δ) in ppm between CH_2 and the OH peaks, determined from the ^1H NMR, was found to be 1.49 ppm, which corresponds to 298.73 K. Averaged molecular radii for

complexes [1]Cl and [1]BPh₄ were estimated from X-ray and DFT molecular structures. The calculated molecular volume is defined as the volume inside a contour of 0.001 electrons/Bohr³.

Conductivity measurements were carried out with a CRISON 522 conductimeter, connected to a conductivity cell CRISON 52 92 with platinum electrodes. The solutions of the complexes (10⁻³ M, in acetonitrile) were prepared in 5 mL volumetric flasks and measured in test tubes. Mass spectra (FAB+) were recorded with a Thermo MAT95XP with a magnetic sector or a Micromass AutoSpec mass spectrometers. Mercury 3.0 (Build RC5) was used to calculate the characteristic parameters of the structures, such as distances, angles, planes, etc. Single crystals were grown by assorted methods. The ligands 2-(2'-hydroxyphenyl)-benzimidazole (HL1) and 2-(2'-hydroxyphenyl)benzothiazole (HL2) and MeIm were purchased from Merck and used without further purification. EpipIm⁸¹ and the metal precursors [Ru(*p*-cym)Cl₂]₂^{82,83} were prepared according to literature procedures.

X-ray Diffraction studies. Crystals for [1]BPh₄•MeOH, [3]BF₄•H₂O, [5]Cl•CDCl₃•0.5 H₂O and [6]BPh₄•H₂O were mounted on a glass fiber. Intensity measurements were collected at 100K with a Bruker Smart Apex diffractometer and with a Bruker X8 APEX II, with graphite-monochromated MoK_α radiation at 100 K ([1]BPh₄), 173K ([3]BF₄ and [5]Cl) and 290K ([6]BPh₄). A semi-empirical absorption correction was applied with the multi-scan^{84,85} methods. Selected crystallographic data can be found in Table S1. The structures were solved by direct methods^{86,87} and refined by full-matrix least-squares⁸⁸ by means of the WINGX⁸⁹ package. All non-hydrogen atoms were refined with anisotropic displacement parameters except those ones of the methanol solvent for compound [1]BPh₄. Hydrogen atoms were geometrically calculated and refined by the riding mode, including the isotropic displacement parameters. The methanol solvent for [1]BPh₄ was modelled as a three-fold disorder with restrained bond distance and two

common isotropic displacement parameters. For [3]BF₄ and [5]Cl, the hydrogen atoms bonded to H₂O molecules have been located in a Fourier synthesis and then fixed. CCDC deposition numbers for [1]BPh₄, [3]BF₄, [5]Cl and [6]BPh₄ are 2012484-2012487.

DFT studies on complexes [1]BPh₄, [1]Cl, [1]OTf, [1]BF₄, and [2]Cl. The DFT calculations were carried out with the Gaussian 09⁹⁰ program package, using the B3LYP-D3 hybrid functional.⁹¹⁻⁹⁴ Geometry optimizations were performed in the gas phase with the LanL2TZ(f) effective core potential basis set for the ruthenium atoms, and the 6-311G(d,p) basis set for the remaining ones

Cell culture. HeLa cells, a human cervical carcinoma cell line, were grown in a humidified atmosphere of 95% air, 5% CO₂ at 37 °C and maintained in Dulbecco's minimal essential medium (Invitrogen, Spain) supplemented with 10% fetal bovine serum as previously described.⁹⁵

Cytotoxicity assays in HeLa cancer cells. Cells were seeded (10⁴ cells/well) and grown in 96-well tissue culture plate. After 24 h, cells were treated with different compounds (1 - 500 μM) for 24 h and 48 h. After treatment, cells were incubated with 0.3 mg/ml XTT solution (sodium 3'-[1-(phenylaminocarbonyl)-3,4-tetrazolium]-bis (4-methoxy-6-nitro) benzene sulfonic acid hydrate) for 30 minutes at 37 °C in control or compound-treated conditions. The cleavage of XTT to form an orange formazan dye by viable cells was monitored by reading absorbance at 475 nm and 690 nm according to the manufacturer's protocol (Cell Proliferation Kit II, Roche, Mannheim, Germany). Three independent experiments carried out in triplicate.

Statistical and data analysis. Non linear regression analysis for IC₅₀ measurements were performed with GraphPad Prism 7.0 program (GraphPad Software, San Diego, CA, USA).

Synthesis and characterization of the new complexes: see Supporting Information.

ASSOCIATED CONTENT

Supporting Information. cif files. x,y,z files from DFT calculations. Synthesis and characterization of the new complexes. Information from X-ray diffraction studies: crystal data, ORTEPs, tables and figures for weak interactions. Tables of ^1H NMR chemical shifts. Table and representations from cytotoxicity studies. Mono and bidimensional NMR spectra of the new complexes. The following files are available free of charge.

AUTHOR INFORMATION

Corresponding Authors

Blanca R. Manzano, U. de Castilla-La Mancha. Departamento de Química Inorgánica, Orgánica y Bioquímica. IRICA. Fac. de Ciencias y Tecnologías Químicas, Avda. C. J. Cela, 10, 13071-Ciudad Real, Spain.

ORCID number: 0000-0002-4908-4503

Email. blanca.manzano@uclm.es

Cristina Tejel. Departamento de Química Inorgánica, Instituto de Síntesis Química y Catálisis Homogénea (ISQCH), CSIC-Universidad de Zaragoza, Pedro Cerbuna 12, 50009-Zaragoza, Spain.

Email. ctejel@unizar.es

ORCID number: 0000-0003-3306-0635

Gustavo Espino, U. de Burgos. Departamento de Química, Facultad de Ciencias. Plaza Misael Bañuelos s. n., 09001-Burgos, Spain.

Email.gespino@ubu.es

ORCID number: 0000-0001-5617-5705

Present Addresses

Present address of Marta Martínez-Alonso: Chimie ParisTech, PSL University, CNRS, Institute of Chemistry for Life and Health Sciences, Laboratory for Inorganic Chemical Biology, 75005 Paris, France

Author Contributions

The manuscript was written through contributions of all authors. All authors have given approval to the final version of the manuscript.

ACKNOWLEDGMENT

This work has been funded by the Spanish Ministerio de Ciencia, Innovación y Universidades (RTI2018-100709-B-C21) and MINECO/FEDER/AGE (CTQ2017-83421-P, C.T.), Junta de Castilla y León (BU087G19) and Gobierno de Aragón/FEDER (GA/FEDER, Inorganic Molecular Architecture Group E08_17R; C.T.) as well as by UCLM (grants 2019-GRIN-27183 and 2019-GRIN-27209) and Junta de Comunidades de Castilla-La Mancha (JCCM) (grant SBPLY/19/180501/000260), both cofinanced with the European Union FEDER. The ‘Centro de Supercomputación de Galicia (CESGA)’ is also gratefully acknowledged for generous allocation of time.

REFERENCES

- (1) Marcus, Y.; Hefter, G. Ion Pairing. *Chem. Rev.* **2006**, *106*, 4585–4621.
- (2) Macchioni, A. Ion Pairing in Transition-Metal Organometallic Chemistry. *Chem. Rev.* **2005**, *105*, 2039–2073.
- (3) Llewellyn, D. B.; Adamson, D.; Arndtsen, B. A. A Novel Example of Chiral Counteranion Induced Enantioselective Metal Catalysis: The Importance of Ion-Pairing in Copper-Catalyzed Olefin Aziridination and Cyclopropanation. *Org. Lett.* **2000**, *2*, 4165–4168.
- (4) Abramo, G. P.; Li, L.; Marks, T. J. Polynuclear Catalysis: Enhancement of Enchainment Cooperativity between Different Single-Site Olefin Polymerization Catalysts by Ion Pairing with a Binuclear Cocatalyst. *J. Am. Chem. Soc.* **2002**, *124*, 13966–13967.
- (5) Brak, K.; Jacobsen, E. N. Asymmetric Ion-Pairing Catalysis. *Angew. Chemie - Int. Ed.* **2013**, *52*, 534–561.
- (6) Goossens, K.; Lava, K.; Bielawski, C. W.; Binnemans, K. Ionic Liquid Crystals: Versatile Materials. *Chem. Rev.* **2016**, *116*, 4643–4807.
- (7) Jaglenc, D.; Dobrzycki, Ł.; Karbarz, M.; Romański, J. Ion-Pair Induced Supramolecular Assembly Formation for Selective Extraction and Sensing of Potassium Sulfate. *Chem. Sci.* **2019**, *10*, 9542–9547.
- (8) Tanaka, H.; Haketa, Y.; Bando, Y.; Yamakado, R.; Yasuda, N.; Maeda, H. Ion-Pairing Assemblies of Porphyrin–Au(III) Complexes in Combination with π -Electronic Receptor–Anion Complexes. *Chem. - An Asian J.* **2020**, 494–498.

- (9) Braga, D.; Grepioni, F.; Desiraju, G. R.; Interactions, I. A. Crystal Engineering and Organometallic Architecture. *Chem. Rev.* **1998**, *98*, 1375–1405.
- (10) Beer, P. D.; Gale, P. A. Anion Recognition and Sensing : The State of the Art and Future Perspectives. *Angew. Chem. Int. Ed.* **2001**, *40*, 486–516.
- (11) Martínez-García, H.; Morales, D.; Pérez, J.; Puerto, M. Interaction between Anions and Cationic Metal Complexes Containing Tridentate Ligands with Exo-C-H Groups : Complex Stability and Hydrogen Bonding. *Chem. Eur. J.* **2014**, *20*, 5821–5834.
- (12) Sutton, L. R.; Scheloske, M.; Pirner, K. S.; Hirsch, A.; Guldi, D. M.; Gisselbrecht, J. P. Unexpected Change in Charge Transfer Behavior in a Cobalt(II) Porphyrin-Fullerene Conjugate That Stabilizes Radical Ion Pair States. *J. Am. Chem. Soc.* **2004**, *126*, 10370–10381.
- (13) Ward, W. M.; Farnum, B. H.; Siegler, M.; Meyer, G. J. Chloride Ion-Pairing with Ru(II) Polypyridyl Compounds in Dichloromethane. *J. Phys. Chem. A* **2013**, *117*, 8883–8894.
- (14) Choi, M. M. F.; Douglas, A. D.; Murray, R. W. Ion-Pair Chromatographic Separation of Water-Soluble Gold Monolayer-Protected Clusters. *Anal. Chem.* **2006**, *78*, 2779–2785.
- (15) Diaz-Torres, R; Alvarez, S. Coordinating Ability of Anions and Solvents towards Transition Metals and Lanthanides. *Dalton Trans.* **2011**, *40*, 10742–10750.
- (16) Hefter, G. When Spectroscopy Fails: The Measurement of Ion Pairing. *Pure Appl. Chem.* **2006**, *78*, 1571–1586.
- (17) Sun, H.; Liu, S.; Lin, W.; Zhang, K. Y.; Lv, W.; Huang, X.; Huo, F.; Yang, H.; Jenkins, G.; Zhao, Q.; et al. Smart Responsive Phosphorescent Materials for Data Recording and

- Security Protection. *Nat. Commun.* **2014**, *5*, 1–9.
- (18) Pregosin, P. S. NMR Spectroscopy and Ion Pairing: Measuring and Understanding How Ions Interact. *Pure Appl. Chem.* **2009**, *81*, 615–633.
- (19) Pregosin, P. S. Applications of NMR Diffusion Methods with Emphasis on Ion Pairing in Inorganic Chemistry : A Mini-Review. *Magn. Reson. Chem.* **2017**, *55*, 405–413.
- (20) Brand, T.; Cabrita, E. J.; Berger, S. Intermolecular Interaction as Investigated by NOE and Diffusion Studies. *Prog. Nucl. Magn. Reson. Spectrosc.* **2005**, *46*, 159–196.
- (21) Bellachioma, G.; Ciancaleoni, G.; Zuccaccia, C.; Zuccaccia, D.; Macchioni, A. NMR Investigation of Non-Covalent Aggregation of Coordination Compounds Ranging from Dimers and Ion Pairs up to Nano-Aggregates. *Coord. Chem. Rev.* **2008**, *252*, 2224–2238.
- (22) Zuccaccia, C.; Macchioni, A.; Orabona, I.; Ruffo, F. Interionic Solution Structure of [PtMe(η^2 -Olefin)(N,N-Diimine)]BF₄ Complexes by ¹⁹F{¹H}-HOESY NMR Spectroscopy: Effect of the Substituents on the Accessibility of the Counterion to the Metal. *Organometallics* **1999**, *18*, 4367–4372.
- (23) Aldrich, K. E.; Billow, B. S.; Holmes, D.; Bemowski, R. D.; Odom, A. L. Weakly Coordinating yet Ion Paired: Anion Effects on an Internal Rearrangement. *Organometallics* **2017**, *36*, 1227–1237.
- (24) Macchioni, A. Ion Pairing in Transition-Metal Organometallic Chemistry. *Chem. Rev.* **2005**, *105*, 2039–2073.
- (25) Müller-Dethlefs, K.; Hobza, P. Noncovalent Interactions : A Challenge for Experiment and Theory. *Chem. Rev.* **2000**, *100*, 143–167.

- (26) Desiraju, G. R.; T. Steiner, T. *The Weak Hydrogen Bond*; Oxford University Press, 2001.
- (27) Jeffrey, G. A. *An Introduction to Hydrogen Bonding*; Oxford University Press: New York, 1997.
- (28) Arunan, E.; Desiraju, G. R.; Klein, R. A.; Sadlej, J.; Scheiner, S.; Alkorta, I.; Clary, D. C.; Crabtree, R. H.; Dannenber, J. J.; Hobza, P.; et al. Definition of the Hydrogen Bond (IUPAC Recommendations 2011). *Pure Appl. Chem.* **2011**, 83, 1637–1641.
- (29) Mautner, M. M. The Ionic Hydrogen Bond. *Chem. Rev.* **2005**, 105, 213–284.
- (30) Steiner, T. The Hydrogen Bond in the Solid State. *Angew. Chem. Int. Ed.* **2002**, 41, 48–76.
- (31) Janiak, C. A Critical Account on π – π Stacking in Metal Complexes with Aromatic Nitrogen-Containing Ligands. *J. Chem. Soc. Dalton Trans.* **2000**, No. 21, 3885–3896.
- (32) Schottel, B. L.; Chifotides, H. T.; Dunbar, K. R. Anion- π Interactions. *J. Chem. Soc. Dalton Trans.* **2008**, 37, 68–83.
- (33) Nishio, M. CH / π Hydrogen Bonds in Crystals. *CrystEng Comm* **2004**, 6, 130–158.
- (34) Nishio, M. The CH/ π Hydrogen Bond in Chemistry. Conformation, Supramolecules, Optical Resolution and Interactions Involving Carbohydrates. *Phys. Chem. Chem. Phys.* **2011**, 13873–13900.
- (35) Tsuzuki, S.; Fujii, A. Nature and Physical Origin of CH/ π Interaction: Significant Difference from Conventional Hydrogen Bonds W. *Phys. Chem. Chem. Phys.* **2008**, 10, 2584–2594.
- (36) Quiñonero, D.; Deyà, P. M.; Carranza, M. P.; Rodríguez, A. M.; Jalón, F. A.; Manzano, B.

- R. Experimental and Computational Study of the Interplay between C-H/ π and Anion- π Interactions. *Dalton Trans.* **2010**, 39, 794–806.
- (37) Berners-Price, S. J.; Girard, G. R.; Hill, D. T.; Sutton, B. M.; Jarrett, P. S.; Faucette, L. F.; Johnson, R. K.; Mirabelli, C. K.; Sadler, P. J. Cytotoxicity and Antitumor Activity of Some Tetrahedral Bis(Diphosphino) Gold(I) Chelates. *J. Med. Chem.* **1990**, 33, 1386–1392.
- (38) Puckett, C. A.; Barton, J. K. Methods to Explore Cellular Uptake of Ruthenium Complexes. *J. Am. Chem. Soc.* **2007**, 129, 46–47.
- (39) Puckett, C. A.; Barton, J. K. Fluorescein Redirects a Ruthenium - Octaarginine Conjugate to the Nucleus. *J. Am. Chem. Soc.* **2009**, 131, 8738–8739.
- (40) Singh, P.; Wang, F.; Hoppel, C. L.; Sayre, L. M. Inhibition of Mitochondrial Respiration by Neutral, Monocationic, and Dicationic Bis-Pyridines Related to the Dopaminergic Neurotoxin 1 -Methyl-4- Phenylpyridinium Cation (MPP⁺). *Arch. Biochem. Biophys.* **1991**, 286, 138–146.
- (41) Sayre, M.; Wang, F.; Hoppel, L. Tetraphenylborate Potentiates the Respiratory Inhibition by the Dopaminergic Neurotoxin MPP⁺ in Both Electron Transport Particles and Intact Mitochondria. *Biochem. Bioph. Res. Co.* **1989**, 161, 809–818.
- (42) Berson, A.; Descatoire, V.; Sutton, A.; Fau, D.; Maulny, B.; Vadrot, N.; Feldmann, G.; Berthon, B.; Tordjmann, T.; Pessayre, D. Toxicity of Alpidem, a Peripheral Benzodiazepine Receptor Ligand, but Not Zolpidem, in Rat Hepatocytes: Role of Mitochondrial Permeability Transition and Metabolic Activation. *J. Pharmacol. Exp.*

Ther. **2001**, 299, 793–800.

- (43) Magut, P. K. S.; Das, S.; Fernand, V. E.; Losso, J.; Mcdonough, K.; Naylor, B. M.; Aggarwal, S.; Warner, I. M. Tunable Cytotoxicity of Rhodamine 6G via Anion Variations. *J. Am. Chem. Soc.* **2013**, 135, 15873–15879.
- (44) Loughrey, B. T.; Healy, P. C.; Parsons, P. G.; Williams, M. L. Selective Cytotoxic Ru(II) Arene Cp* Complex Salts $[R-PhRuCp^*]^+ X^-$ for $X = BF_4^-, PF_6^-$, and BPh_4^- . *Inorg. Chem.* **2008**, 47, 8589–8591.
- (45) Santos, D. L.; Golbaghi, G.; Haghdoost, M. M.; Yancu, D.; Lo, Y.; Doucet, N.; Patten, S. A.; Sanderson, J. T.; Castonguay, A. Organoruthenium(II) Complexes Bearing an Aromatase Inhibitor: Synthesis, Characterization, in Vitro Biological Activity and in Vivo Toxicity in Zebra Fish Embryos. *Organometallics* **2019**, 38, 702–711.
- (46) Haghdoost, M. M.; Golbaghi, G.; Guard, J.; Sielanczyk, S.; Patten, S. A.; Castonguay, A. Synthesis, Characterization and Biological Evaluation of Cationic Organoruthenium(II) Fluorene Complexes: Influence of the Nature of the Counteranion. *Dalton Trans.* **2019**, 48, 13396–13405.
- (47) Zhang, H.; Guo, L.; Tian, Z.; Tian, M.; Zhang, S.; Xu, Z.; Gong, P.; Zheng, X.; Zhao, J.; Liu, Z. Anticancer Activity of Iridium(III) Complexes. *Chem. Commun.* **2018**, 54, 4421–4424.
- (48) Milcic, K.; Tomic, Z. D.; Zaric, S. D. Very Strong Metal Ligand Aromatic Cation- p Interactions in Transition Metal Complexes: Intermolecular Interaction in Tetraphenylborate Salts. *Inorg. Chim. Acta* **2004**, 357, 4327–4329.

- (49) Kumita, H.; Kato, T.; Jitsukawa, K.; Einaga, H.; Masuda, H. Characterization of an NH- π Interaction in Co(III) Ternary Complexes with Aromatic Amino Acids. *Inorg. Chem.* **2001**, *40*, 3936–3942.
- (50) Hall, B. R.; Manck, L. E.; Tidmarsh, I. S.; Stephenson, A.; Taylor, B. F.; Blaikie, E. J.; Griend, A. Vander; Ward, M. D. Structures, Host – Guest Chemistry and Mechanism of Stepwise Self-Assembly of M₄L₆ Tetrahedral Cage Complexes. *J. Chem. Soc. Dalton Trans.* **2011**, *40*, 12132–12145.
- (51) Arata, X.; Torigoe, H.; Iihoshi, T.; Matsumoto, N.; Dahan, F.; Tuchagues, J.-P. NH/ π Interaction in a Spin-Crossover Complex. *Inorg. Chem.* **2005**, *44*, 9288–9292.
- (52) Aliende, C.; Pérez-Manrique, M.; Jalón, F. A.; Manzano, B. R.; Rodríguez, A. M.; Cuevas, J. V.; Espino, G.; Martínez, M. Á.; Massaguer, A.; González-Bártulos, M.; De Llorens, R.; Moreno, V. Preparation of New Half Sandwich Ruthenium Arene Complexes with Aminophosphines as Potential Chemotherapeutics. *J. Inorg. Biochem.* **2012**, *117*, 171–188.
- (53) Mari, C.; Pierroz, V.; Gasser, G. Combination of Ru(II) Complexes and Light: New Frontiers in Cancer Therapy. *Chem. Sci.* **2015**, *6*, 2660–2686.
- (54) Gasser, G.; Ott, I.; Metzler-Nolte, N. Organometallic Anticancer Compounds. *J. Med. Chem.* **2011**, *54*, 3–25.
- (55) Yan, Y. K.; Melchart, M.; Habtemariam, A.; Sadler, P. J. Organometallic Chemistry, Biology and Medicine: Ruthenium Arene Anticancer Complexes. *Chem. Commun.* **2005**, 4764–4776.

- (56) Bergamo, A.; Sava, G. Linking the Future of Anticancer Metal-Complexes to the Therapy of Tumour Metastases. *Chem. Soc. Rev.* **2015**, *44*, 8818–8835.
- (57) Martínez, M.; Carranza, M. P.; Massaguer, A.; Santos, L.; Organero, J. A.; Aliende, C.; De Llorens, R.; Ng-Choi, I.; Feliu, L.; Planas, M.; et al. Synthesis and Biological Evaluation of Ru(II) and Pt(II) Complexes Bearing Carboxyl Groups as Potential Anticancer Targeted Drugs. *Inorg. Chem.* **2017**, *56*, 13679–13696.
- (58) Medici, S.; Peana, M.; Marina, V.; Lachowicz, J. I.; Crisponi, G.; Antonietta, M. Noble Metals in Medicine: Latest Advances. *Coord. Chem. Rev.* **2015**, *284*, 329–350.
- (59) Murray, B. S.; Babak, M. V.; Hartinger, C. G.; Dyson, P. J. The Development of RAPTA Compounds for the Treatment of Tumors. *Coord. Chem. Rev.* **2016**, *306*, 86–114.
- (60) Allardyce, C. S.; Dyson, P. J. Metal-Based Drugs That Break the Rules. *Dalton Trans.* **2016**, *45*, 3201–3209.
- (61) Alessio, E. Thirty Years of the Drug Candidate NAMI-A and the Myths in the Field of Ruthenium Anticancer Compounds: A Personal Perspective. *Eur. J. Inorg. Chem.* **2017**, *2017*, 1549–1560.
- (62) Rathinassmy, S.; Somalingappa, S.; Karki, S.; Bhattacharya, S.; Manikandan, L.; Prabakaran, S. G.; Gupta, M. . M. U. K. Synthesis and Anticancer Activity of Certain Mononuclear Ru(II) Complexes. *J. Enz. Inh. Med. Chem.* **2006**, *21*, 501–507.
- (63) Lari, M.; Martínez-Alonso, M.; Busto, N.; Manzano, B. R.; Rodríguez, A. M.; Acuna, M. I.; Domínguez, F.; Albasanz, J. L.; Leal, J. M.; Espino, G.; et al. Strong Influence of Ancillary Ligands Containing Benzothiazole or Benzimidazole Rings on Cytotoxicity and

- Photoactivation of Ru(II) Arene Complexes. *Inorg. Chem.* **2018**, *57*, 14322–14336.
- (64) Marcus, Y. Thermodynamics of Solvation of Ions. Part 5.—Gibbs Free Energy of Hydration at 298.15 K. *J. Chem. Soc. Faraday Trans* **1991**, *87*, 2995–2999.
- (65) Pastuszko, A.; Majchrzak, K.; Czyz, M.; Budzisz, E. The Synthesis, Lipophilicity and Cytotoxic Effects of New Ruthenium(II) Arene Complexes with Chromone Derivatives. *J. Inorg. Biochem.* **2016**, *159*, 133–141.
- (66) Martin, R. B. *Cisplatin Chemistry and Biochemistry of a Leading Anticancer Drug*; Verlag Helvetica Chimica Acta: Zurich, 2006.
- (67) Carrión, M. C.; Jalón, F. A.; Manzano, B. R.; Rodríguez, A. M.; Sepúlveda, F.; Maestro, M. (Arene)Ruthenium(II) Complexes Containing Substituted Bis(Pyrazolyl)Methane Ligands - Catalytic Behaviour in Transfer Hydrogenation of Ketones. *Eur. J. Inorg. Chem.* **2007**, 3961–3973.
- (68) Carrión, M. C.; Sepúlveda, F.; Jalón, F. A.; Manzano, B. R.; Rodríguez, A. M. Base-Free Transfer Hydrogenation of Ketones Using Arene Ruthenium(II) Complexes. *Organometallics* **2009**, *28*, 3822–3833.
- (69) Vock, C. A.; Scolaro, C.; Phillips, A. D.; Scopelliti, R.; Sava, G.; Dyson, P. J. Synthesis , Characterization , and in Vitro Evaluation of Novel Ruthenium (II) η^6 -Arene Imidazole Complexes. *J. Med. Chem.* **2006**, *49*, 5552–5561.
- (70) Bugarcic, T.; Habtemariam, A.; Stepankova, J.; Heringova, P.; Kasparkova, J.; Deeth, R. J.; Johnstone, R. D. L.; Prescimone, A.; Parkin, A.; Parsons, S.; et al. The Contrasting Chemistry and Cancer Cell Cytotoxicity of Bipyridine and Bipyridinediol Ruthenium(II)

- Arene Complexes. *Inorg. Chem.* **2008**, *47*, 11470–11486.
- (71) Patel, A. K.; Mishra, S. K.; Krishnamurthy, K.; Suryaprakash, N. Retention of Strong Intramolecular Hydrogen Bonds in High Polarity Solvents in Binaphthalene-Benzamide Derivatives: Extensive NMR Studies. *RSC Adv.* **2019**, *9*, 32759–32770.
- (72) Martínez-Alonso, M.; Busto, N.; Jalón, F. A.; Manzano, B. R.; Leal, J. M.; Rodríguez, A. M.; García, B.; Espino, G. Derivation of Structure – Activity Relationships from the Anticancer Properties of Ruthenium(II) Arene Complexes with 2-Aryldiazole Ligands. *Inorg. Chem.* **2014**, *53*, 11274–11288.
- (73) Ammer, J.; Nolte, C.; Karaghiosoff, K.; Thallmair, S.; Mayer, P.; Devivie-Riedle, R.; Mayr, H. Ion-Pairing of Phosphonium Salts in Solution: C-H \cdots halogen and C-H $\cdots\pi$ Hydrogen Bonds. *Chem. - A Eur. J.* **2013**, *19*, 14612–14630.
- (74) Dupont, J.; Suarez, P. A. Z.; De Souza, R. F.; Burrow, R. A.; Kintzinger, J. P. C-H- π Interactions in 1-n-Butyl-3-Methylimidazolium Tetraphenylborate Molten Salt: Solid and Solution Structures. *Chem. - Eur. J.* **2000**, *6*, 2377–2381.
- (75) Zuccaccia, D.; Macchioni, A. An Accurate Methodology to Identify the Level of Aggregation in Solution by PGSE NMR Measurements: The Case of Half-Sandwich Diamino Ruthenium(II) Salts. *Organometallics* **2005**, *24*, 3476–3486.
- (76) MacChioni, A.; Ciancaleoni, G.; Zuccaccia, C.; Zuccaccia, D. Determining Accurate Molecular Sizes in Solution through NMR Diffusion Spectroscopy. *Chem. Soc. Rev.* **2008**, *37*, 479–489.
- (77) Zuccaccia, C.; Bellachioma, G.; Cardaci, G.; Macchioni, A. Self-Diffusion Coefficients of

- Transition-Metal Complex Ions, Ion Pairs, and Higher Aggregates by Pulsed Field Gradient Spin - Echo NMR Measurements. *Organometallics* **2000**, *19*, 4663–4665.
- (78) Zuccaccia, D.; Sabatini, S.; Bellachioma, G.; Cardaci, G.; Clot, E.; Macchioni, A. PGSE and NOE NMR Evidence for Higher Order Aggregation in Some Cationic Ruthenium Complexes in Both Protic and Aprotic Solvents. *Inorg. Chem.* **2003**, *42*, 5465–5467.
- (79) Zuccaccia, D.; Bellachioma, G.; Cardaci, G.; Ciancaleoni, G.; Zuccaccia, C.; Clot, E.; Macchioni, A. Interionic Structure of Ion Pairs and Ion Quadruples of Half-Sandwich Ruthenium(II) Salts Bearing Alfa-Diimine Ligands. *Organometallics* **2007**, *26*, 3930–3946.
- (80) Pregosin, P. S.; Kumar, P. G. A.; Fernald, I. Pulsed Gradient Spin–Echo (PGSE) Diffusion and ^1H , ^{19}F Heteronuclear Overhauser Spectroscopy (HOESY) NMR Methods in Inorganic and Organometallic Chemistry: Something Old and Something New. *Chem. Rev.* **2005**, *105*, 2977–2998.
- (81) Luo, J.; Xin, T.; Wang, Y. A PEG Bridged Tertiary Amine Functionalized Ionic Liquid Exhibiting Thermoregulated Reversible Biphasic Behavior with Cyclohexane/Isopropanol: Synthesis and Application in Knoevenagel Condensation. *New J. Chem.* **2013**, *37*, 269–273.
- (82) Zelonka, R. A.; Baird, M. C. Benzene Complexes of Ruthenium(II). *Can. J. Chem.* **1972**, *50*, 3063–3072.
- (83) Bennett, M. A.; Smith, A. K. Arene Ruthenium(II) Complexes Formed by Dehydrogenation of Cyclohexadienes with Ruthenium(III) Trichloride. *J. Chem. Soc.*

Dalton Trans. **1974**, No. 2, 233.

- (84) G. M. Sheldrick. *SADABS, Bruker AXS, 1997*.; Madison, WI (USA), 1997.
- (85) Krause, L.; Herbst-Irmer, R.; Sheldrick, G. M.; Stalke, D. Comparison of Silver and Molybdenum Microfocus X-Ray Sources for Single-Crystal Structure Determination. *J. Appl. Crystallogr.* **2015**, *48*, 3–10.
- (86) Burla, M. C.; Camalli, M.; Carrozzini, B.; Cascarano, G. L.; Giacovazzo, C.; Polidori, G.; Spagna, R. SIR2002 : The Program. *J. Appl. Cryst.* **2003**, *36*, 1103.
- (87) Sheldrick, G. M. SHELXT – Integrated Space-Group and Crystal- Structure Determination. *Acta Cryst. A* **2015**, *A71*, 3–8.
- (88) Sheldrick, G. M. A Short History of SHELX. *Acta Cryst.* **2008**, *A64*, 112–122.
- (89) Farrugia, L. J. WinGX and ORTEP for Windows : An Update. *J. Appl. Cryst.* **2012**, *45*, 849–854.
- (90) M. J. Frisch, G. et al 2009. Gaussian 09, R. D. 01. S. supporting information for complete reference. Gaussian 09, Revision D.01.
- (91) Lee, C.; Yang, W.; Parr, R. G. Development of the Colle-Salvetti Correlation-Energy Formula into a Functional of the Electron Density. *Phys. Rev. B* **1988**, *37*, 785–789.
- (92) Becke, A. D. A New Mixing of Hartree-Fock and Local Density-Functional Theories. *J. Chem. Phys.* **1993**, *98*, 1372–1377.
- (93) Becke, A. D. Density-Functional Thermochemistry.III. The Role of Exact Exchange. *J. Chem. Phys.* **1993**, *98*, 5648–5652.

- (94) S. Grimme, J. Antony, S. Ehrlich, H. K. A Consistent and Accurate Ab Initio Parametrization of Density Functional Dispersion Correction (DFT-D) for the 94 Elements H-Pu. *J. Chem. Phys.* **2010**, *132*, 154104.
- (95) Buira, S. P.; Albasanz, J. L.; Dentesano, G.; Moreno, J.; Martín, M.; Ferrer, I.; Barrachina, M. DNA Methylation Regulates Adenosine A2A Receptor Cell Surface Expression Levels. *J. Neurochem.* **2010**, *112*, 1273–1285.

Table of Contents

SYNOPSIS. We have synthesized a set of cationic *p*-cymene ruthenium complexes with a neutral monodentate and an anionic bidentate ligands and different anions. Based on X-ray diffraction studies, DFT calculations and solution NMR studies, it is demonstrated the existence of strong anion-cation interactions ($\text{N-H}\cdots\text{X}$, $\text{X} = \text{Cl}, \text{F}, \text{O}$, and $\text{C-H}\cdots\pi$ interactions) and the formation of intimate ion-pairs and quadruples in solution. The complexes with the BPh_4^- anion are more cytotoxic against Hela cell lines.

